

Measurement of the Neutron Electric Form Factor $G_{E,n}$ in the Quasifree ${}^2\text{H}(\vec{e}, e'\vec{n})p$ Reaction

M. Ostrick,^{1,*} C. Herberg,¹ H. G. Andresen,¹ J. R. M. Annand,² K. Aulenbacher,¹ J. Becker,³ P. Drescher,³ D. Eyl,¹ A. Frey,¹ P. Grabmayr,⁴ P. Hartmann,¹ T. Hehl,⁴ W. Heil,³ J. Hoffmann,³ D. Ireland,² J. D. Kellie,² F. Klein,⁵ K. Livingston,² Ch. Nachtigall,³ A. Natter,⁴ E. W. Otten,³ R. O. Owens,² E. Reichert,³ D. Rohe,³ H. Schmieden,¹ R. Sprengard,¹ M. Steigerwald,³ K.-H. Steffens,¹ Th. Walcher,¹ and R. Watson²

¹Institut für Kernphysik, Universität Mainz, D-55099 Mainz, Germany

²Department of Physics and Astronomy, University of Glasgow, Glasgow, United Kingdom

³Institut für Physik, Universität Mainz, D-55099 Mainz, Germany

⁴Physikalisches Institut, Universität Tübingen, D-72076 Tübingen, Germany

⁵Physikalisches Institut, Universität Bonn, D-53115 Bonn, Germany

(Received 4 December 1998; revised manuscript received 19 March 1999)

The electric form factor of the neutron $G_{E,n}$ has been measured in the quasifree ${}^2\text{H}(\vec{e}, e'\vec{n})p$ reaction using the 855 MeV polarized cw electron beam of the Mainz Microtron MAMI. The polarization of the scattered neutrons was analyzed in a polarimeter consisting of two walls of plastic scintillators. The precession of the neutron spin in a magnetic field was used for the first time to circumvent the measurement of the effective analyzing power of the polarimeter and the beam polarization. In this way $G_{E,n}$ could be determined with little model dependence and experimental uncertainties. The result $G_{E,n}(0.34 \text{ GeV}^2/c^2) = 0.0611 \pm 0.0069_{\text{stat}} \left(\begin{smallmatrix} +0.0069 \\ -0.0055 \end{smallmatrix} \right)_{\text{sys}}$ is larger than previously assumed.

PACS numbers: 14.20.Dh, 13.40.Gp, 24.70.+s, 25.30.-c

The internal structure of protons and neutrons at low energies is still an unsolved problem. At momentum transfers of the order $Q^2 \sim \Lambda_{\text{QCD}}^2$, where $\Lambda_{\text{QCD}} \approx 250 \text{ MeV}^2/c^2$ is the scale parameter of quantum chromodynamics (QCD), perturbative solutions are not possible. Rather, the strictly nonlinear QCD has to be solved in the framework of lattice gauge theory or approximated by effective field theories. Sensitive tests of these solutions require the detailed comparison with low energy observables, such as the excitation spectrum of the nucleon or the electric and magnetic form factors. In particular, the form factors, which are measured by elastic electron-nucleon scattering, contain the information on the spatial distribution of charge and magnetization in the nucleon. The electric form factor of the neutron $G_{E,n}$ is of special significance since the charge of the neutron vanishes and a nonzero form factor must come from a nonuniform spatial distribution of valence quarks or the sea of correlated quark-antiquark pairs, e.g., pions.

The experimental information on $G_{E,n}$ is still unsatisfactory for two reasons. First, the lack of a free neutron target requires the use of nuclear targets thus introducing binding effects. Second, the standard Rosenbluth separation of the longitudinal cross section arising from the electric form factor $G_{E,n}(Q^2)$ and the transverse cross section due to the magnetic form factor $G_{M,n}(Q^2)$ in

$$\frac{d\sigma}{d\Omega} = \frac{\sigma_{\text{Mott}}}{\epsilon(1+\tau)} \frac{E'}{E} (\epsilon G_{E,n}^2 + \tau G_{M,n}^2)$$

are limited because $G_{E,n}^2(Q^2) \ll \tau G_{M,n}^2(Q^2)$. Here σ_{Mott} denotes the Mott cross section, $\tau = Q^2/4M^2$, and $\epsilon = [1 + 2(1 + \tau) \tan^2 \vartheta_e/2]^{-1}$. Recently, such a separation of $G_{E,n}$ in the range $Q^2 \approx 1.75\text{--}4 \text{ GeV}^2/c^2$ yielded data compatible with $G_{E,n} \equiv 0$ [1].

More precise data at lower momentum transfers ($Q^2 < 1 \text{ GeV}^2/c^2$) came from the study of the deuteron structure function $A(Q^2)$, measured in elastic electron-deuteron scattering. $A(Q^2)$ provides a higher sensitivity to $G_{E,n}$ through the mixed term $G_{E,n}G_{E,p}$ in the square of the isoscalar form factor $(G_{E,n} + G_{E,p})^2$. However, the necessary unfolding of the deuteron wave function introduces a substantial model dependence in $G_{E,n}$ ([2,3] and Fig. 4).

A more promising approach to measure $G_{E,n}$ is offered by the use of polarization observables. For elastic $n(\vec{e}, e'\vec{n})$ scattering of longitudinally polarized electrons the polarization of the recoiling neutron is given in the (x, y, z) frame of Fig. 1 by [4]

$$\begin{aligned} \vec{P}^n &= hP_e(P_x^n \hat{e}_x + P_y^n \hat{e}_y + P_z^n \hat{e}_z) \\ &= \frac{hP_e}{\epsilon G_E^2 + \tau G_M^2} \left[-\sqrt{2\tau\epsilon(1-\epsilon)} G_{E,n} G_{M,n} \hat{e}_x \right. \\ &\quad \left. + \tau\sqrt{1-\epsilon^2} G_{M,n}^2 \hat{e}_z \right], \end{aligned} \quad (1)$$

where P_e denotes the absolute value of the electron polarization and $h = \pm 1$ the electron helicity. In the ratio P_x^n/P_z^n the unpolarized cross section as well as the electron

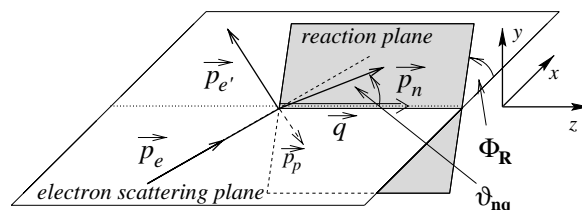


FIG. 1. (x, y, z) reference frame and kinematics of the ${}^2\text{H}(\vec{e}, e'\vec{n})p$ reaction.

polarization P_e cancels out providing a sensitive experimental access to the ratio $G_{E,n}/G_{M,n}$,

$$\frac{P_x^n}{P_z^n} = \frac{-\sqrt{2\epsilon}}{\sqrt{\tau(1+\epsilon)}} \frac{G_{E,n}}{G_{M,n}}. \quad (2)$$

However, when using light nuclei as neutron targets one still has to pay attention to nuclear binding effects. In first order (i.e., plane wave Born approximation, no final state interactions) the scattering from the neutron and the spectral function factorize in the cross section so that the latter cancels in the polarization components given by Eq. (1). In studying the details of the reaction Arenhövel [5] has shown that in the case of a deuteron target meson exchange and isobar currents have a negligible effect in quasifree kinematics as does the choice of the N - N potential so that there is essentially no dependence on the deuteron wave function. Within these calculations final state interactions (FSI) lead to a relative reduction of the neutron polarization of less than 4% at $Q^2 \approx 0.35 \text{ GeV}^2/c^2$. At lower momentum transfer a strongly rising influence of FSI, especially of charge exchange reactions, is found [6] and has been included in the systematic error. A detailed study of the kinematic dependence of FSI along with a measurement of $G_{E,n}$ at $Q^2 < 0.2 \text{ GeV}^2/c^2$ will be presented in a forthcoming paper [7]. A real experiment cannot be restricted to the strictly quasifree case ($\vartheta_{nq} = 0$) but will cover a finite range in ϑ_{nq} and Φ_R (Fig. 1). Finite angles ϑ_{nq} and Φ_R correspond to the so-called Wigner rotation [8] of the quantization axes and lead to a mixing of the polarization components P_x^n and P_z^n which averages out in case of an azimuthally symmetric event population. A comparison with the calculations of Arenhövel *et al.* shows that this mixing dominates the ϑ_{nq} and Φ_R dependence of the neutron polarization for angles $\vartheta_{nq} < 10^\circ$ at $Q^2 > 0.2 \text{ GeV}^2/c^2$ [9].

This Letter presents a determination of $G_{E,n}$ at $Q^2 = 0.34 \text{ GeV}^2/c^2$ using the ${}^2\text{H}(\vec{e}, e'\vec{n})p$ reaction and the 855 MeV, longitudinally polarized cw beam of the Mainz Microtron MAMI [10]. The polarized-electron source is based on photoelectron emission of GaAsP [11]. At the cylindrical, 5 cm thick, liquid deuterium target an average beam current of $2 \mu\text{A}$ was available with a typical polarization of $\overline{P_e} = 75\%$. The helicity of the beam was reversed during the experiment with a frequency of 1 Hz to eliminate instrumental asymmetries. The electron polarization was measured at the source (100 keV) with a Mott polarimeter and before the target (855 MeV) by Møller scattering. A bremsstrahlung-transmission Compton polarimeter, situated in the electron beam dump, provided continuous monitoring of beam polarization throughout the experiment [12].

The detector setup is shown schematically in Fig. 2. The scattered electrons were detected in a segmented Pb-glass calorimeter with an angular resolution of $\delta\vartheta_e \approx \delta\varphi_e < \pm 0.2^\circ$. The energy resolution of $\delta E/E \approx 20\%$ was sufficient to suppress inelastic events resulting from

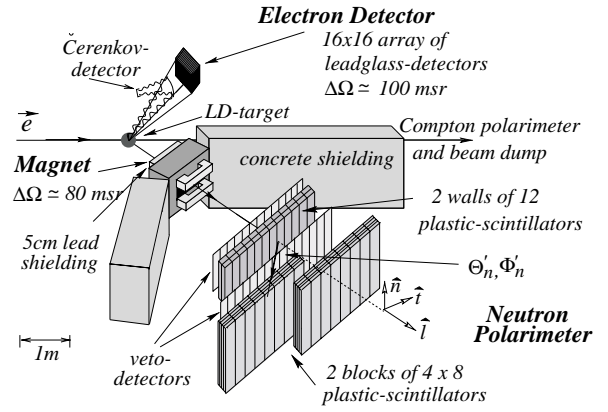


FIG. 2. Detector setup and the $(\hat{i}, \hat{n}, \hat{l})$ reference frame in the neutron scattering plane defined by the neutron momentum and the beam direction.

π production by rejecting events with a pulse height below 90% of the quasielastic peak position (i.e., below 600 MeV typically). This was cross-checked using a high resolution bismuth germanate BaF_2 calorimeter with reduced solid angle and a beam current of a few nA [13]. The neutrons were detected in coincidence with the electrons by two large area walls of plastic scintillators well shielded by concrete and by 5 cm thick lead. The first wall [14] consisted of 24 vertical bars each equipped with photomultipliers on both ends and operated as a time of flight spectrometer: $\delta\vartheta_n \approx \pm 1.5^\circ$; $\delta\varphi_n < \pm 1.0^\circ$; $\delta\beta_n/\beta_n \approx 6\%$ (FWHM) for neutron energies relevant in this experiment. The kinematic observables ϑ_e , φ_e , ϑ_n , φ_n , and β_n were used for the reconstruction of the three-body final state. The measured energy of the scattered electrons provided no further constraint in this respect because of its larger uncertainty. The systematic error for the reconstructed direction of the momentum transfer ($\delta\Theta_q^{\text{sys}} \approx \pm 0.4^\circ$) is then dominated by systematic uncertainties in the measurement of the neutron time of flight. The contribution of $p \rightarrow n$ charge exchange reactions in the lead shielding to the yield of neutrons that satisfies all kinematical conditions was determined experimentally to be smaller than 1.5% using a liquid hydrogen target [15]. Applying the spin-transfer coefficients for the free $\vec{p} \rightarrow \vec{n}$ scattering [16] to this neutron sample results in a modification of P_x^n/P_z^n by 1%. A possible depolarization of neutrons in lead was investigated by Eden *et al.* [17] and no significant effects were found.

For the analysis of the neutron polarization the detection process itself can be used. As has been demonstrated by Taddeucci *et al.* [18], np scattering in plastic scintillators offers a reasonable analyzing power $\mathcal{A}_{\text{eff}}(\Theta'_n, T_n) \approx 20\% - 40\%$ at neutron energies from 100 to 200 MeV leading to an asymmetry in the azimuthal angle, Φ_n , of the secondary scattered neutrons,

$$N^h(\Theta'_n, \Phi'_n) = N_0(1 + hP_e \mathcal{A}_{\text{eff}}(\Theta'_n, T_n) \times [P_x^n \sin\Phi'_n + P_z^n \cos\Phi'_n]).$$

P_t^n and P_z^n [$(\hat{t}, \hat{n}, \hat{l})$ frame in Fig. 2] denote the polarization components with respect to the neutron scattering plane perpendicular to the direction of the neutron momentum. In the case $\vartheta_{nq} = 0$ they are given by P_x^n and

P_y^n , respectively. The scattering angles Θ'_n and Φ'_n can be reconstructed through the hit position in the second scintillator wall [19]. The Φ'_n asymmetry $A(\Phi'_n)$ was determined through the ratio

$$A(\Phi'_n) = \frac{\sqrt{N^+(\Phi'_n)N^-(\Phi'_n + \pi)} - \sqrt{N^-(\Phi'_n)N^+(\Phi'_n + \pi)}}{\sqrt{N^+(\Phi'_n)N^-(\Phi'_n + \pi)} + \sqrt{N^-(\Phi'_n)N^+(\Phi'_n + \pi)}} \equiv a_t^n \sin\Phi'_n + a_n^n \cos\Phi'_n$$

in which the detector efficiencies and helicity dependent luminosity fluctuations cancel. The determination of the desired neutron recoil polarization from the amplitudes $a_t^n = P_e \mathcal{A}_{\text{eff}} P_t^n$ and $a_n^n = P_e \mathcal{A}_{\text{eff}} P_z^n$ requires the knowledge of the effective analyzing power \mathcal{A}_{eff} of the polarimeter which depends crucially on the kinematic cuts applied to select the np -scattering events in the first detector plane. An absolute calibration can be circumvented by measuring the ratio $a_t^n/a_n^n = P_t^n/P_z^n$ in which the analyzing power as well as the electron polarization cancel. Therefore, the longitudinal polarization component P_z^n has also to be determined. This was achieved by using the spin precession in a magnetic field. On their path L through a dipole magnet with a vertical field $\vec{B} = B\hat{n}$ the neutron spins precess through the angle

$$\chi = \frac{-1.91e}{m_p \beta_n c} \int_L B(l) dl \quad (3)$$

in the neutron scattering plane due to their anomalous magnetic moment $\mu_n = -1.91\mu_K$. The field integral $|\int B(l) dl|$ was varied between 0.15 Tm ($|\chi| \approx 10^\circ$) and 1.3 Tm ($|\chi| \approx 90^\circ$) and was measured to an accuracy of 0.005 Tm over the whole acceptance of the magnet. In the data analysis only events with precession angles deviating by less than 1% from Eq. (3) due to nonvertical field components were accepted. After the precession by χ the transverse amplitude $a_t^n(\chi)$ receives contributions from both P_t^n and P_z^n ,

$$a_t^n(\chi) = P_e \mathcal{A}_{\text{eff}} (P_t^n \cos\chi - P_z^n \sin\chi) \equiv A_0 \sin(\chi - \chi_0). \quad (4)$$

The angle of zero crossing of the amplitude a_t^n , χ_0 , is directly related to the ratio of the polarization components and depends neither on the analyzing power of the polarimeter nor on the polarization of the electron beam

$$\tan\chi_0 = \frac{P_e \mathcal{A}_{\text{eff}} P_t^n}{P_e \mathcal{A}_{\text{eff}} P_z^n}.$$

Asymmetry data for various precession angles χ are shown in Fig. 3. Kinematic cuts on the analyzing reaction change the amplitude of a_t^n (i.e., the effective analyzing power) but not the zero crossing angle χ_0 . This has been investigated for a variety of different conditions [7,9]. On the other hand, the observed ratio P_t^n/P_z^n in the ${}^2\text{H}(e, e'n)p$ reaction does depend on the degree of deviation from the free $n(e, e'n)$ kinematics, as outlined above. In order to extract the ratio P_x^n/P_z^n [Eq. (2)] from the measured ratio $P_t^n/P_z^n = \tan\chi_0$ the effect of the kinematic acceptance was corrected using the reconstructed reaction kinematics. The relative size of this correction ($\approx -3\%$) is smaller than the systematic error ($\pm 7.5\%$) caused by the uncertainty in the momentum-transfer direction (Θ_q), which is a dominant contribution to the systematic uncertainty (Table I).

The electric form factor can be calculated by means of Eq. (2). For the magnetic form factor the empirical dipole fit $G_{M,n}(Q^2) = \mu_n(1 + Q^2/0.71 \text{ GeV}^2/c^2)^{-2}$ was used. This form has recently been confirmed in the

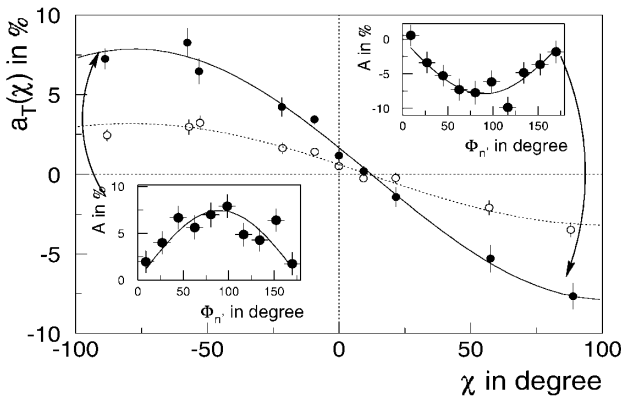


FIG. 3. Measured amplitudes $a_t^n(\chi)$ of reconstructed Φ'_n asymmetries (two examples are given in the insets) for various precession angles χ averaged over the detector acceptance, with two different kinematic cuts on the analyzing np reaction.

TABLE I. Summary of contributions to the systematic error relative to the $G_{E,n}$ value averaged over the whole Q^2 acceptance.

Source	$(\Delta G_{E,n})^{\text{sys}}/G_{E,n}$
Reconstruction of reaction geometry	$\pm 7.5\%$
Final State interactions (FSI)	$+8\%$
Contribution of non-quasi-free events	-4%
Determination of precession angle χ	$\pm 2\%$
Experimental uncertainty in $G_{M,n}$	$\pm 2\%$
Kinematic factor in Eq. (2)	$\pm 1\%$
$p \rightarrow n$ reactions in the lead shielding	$\pm 1\%$
Beam polarization	$\pm 0.5\%$
Square sum	$+11.4\%$
	-9.1%

TABLE II. Results for $G_{E,n}$. The larger systematic uncertainty at low Q^2 is due to the rising influence of FSI [6,7].

Q^2 in GeV^2/c^2	$G_{E,n} \pm (\Delta G_{E,n})^{\text{stat}} \pm (\Delta G_{E,n})^{\text{syst}}$
0.29 ± 0.02	$0.059 \pm 0.011^{+0.013}_{-0.0055}$
0.34 ± 0.03	$0.074 \pm 0.012^{+0.0055}_{-0.0055}$
0.42 ± 0.05	$0.049 \pm 0.013^{+0.0054}_{-0.0055}$
$0.34^{+0.13}_{-0.07}$	$0.0611 \pm 0.0069^{+0.0069}_{-0.0055}$

range $Q^2 \approx 0.3\text{--}0.4 \text{ GeV}^2/c^2$ with a statistical error of 2% [20]. Systematic errors in $G_{M,n}$ are still under discussion [21] and are not included here. According to Eq. (2), any correction of $G_{M,n}$ will propagate linearly into the extracted value for $G_{E,n}$. The extracted values for $G_{E,n}$ in three different Q^2 bins are given in Table II. The result averaged over the whole Q^2 acceptance is shown in Fig. 4 along with results from other double polarization experiments [22–24] and the results extracted from the elastic deuteron response using four different NN potentials [3]. A measurement of $G_{E,n}$ in the ${}^3\text{He}(\vec{\bar{e}}, en)pp$ reaction which was performed with an almost identical detector setup [24] resulted in a significantly lower value. As already mentioned, charge exchange reactions in the final state of the ${}^2\text{H}(\vec{\bar{e}}, e'\vec{n})p$ reaction reduce $P_{\vec{n}}$ significantly at $Q^2 = 0.15 \text{ GeV}^2/c^2$. Because of the much stronger binding of the neutron in ${}^3\text{He}$ this FSI might remain important up to higher values of Q^2 in ${}^3\text{He}(\vec{\bar{e}}, en)pp$. In summary the neutron recoil polarization in ${}^2\text{H}(\vec{\bar{e}}, e'\vec{n})p$ has been measured using the spin precession in a magnetic field for the first time. In this way experimental

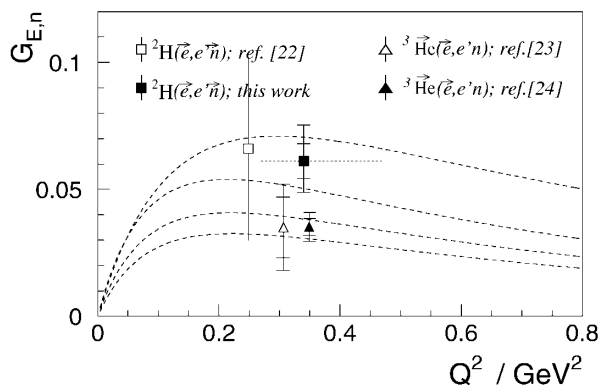


FIG. 4. The result of this work (■) with statistical and systematic errors (vertical bars) and the Q^2 range (horizontal dotted line) with other $G_{E,n}$ measurements in double polarization experiments [21–23] and the best fits to data extracted from the elastic deuteron response using four different NN potentials [3] (dashed lines).

calibration factors could be eliminated and a value for $G_{E,n}$ at $Q^2 = 0.34 \text{ GeV}^2/c^2$ with little residual model dependence was obtained. The result lies at the upper limit of the model dependence in [3] and higher than the preferred result therein.

The authors wish to acknowledge the excellent support of the accelerator group of MAMI, as well as many other scientists and technicians of the Institut für Kernphysik in Mainz. We would also like to thank H. Arenhövel for fruitful discussions. This work was supported by the Deutsche Forschungsgemeinschaft (SFB 201), BMBF(06 TU 669), DAAD, and the U.K. Engineering and Physical Sciences Research Council.

*Present address: Physikalisches Institut, Universität Bonn, D-53115 Bonn, Germany.

- [1] A. Lung *et al.*, Phys. Rev. Lett. **70**, 718 (1993).
- [2] S. Galster *et al.*, Nucl. Phys. **B32**, 221 (1971).
- [3] S. Platchkov *et al.*, Nucl. Phys. **A510**, 740 (1990).
- [4] R. G. Arnold *et al.*, Phys. Rev. C **23**, 363 (1981).
- [5] H. Arenhövel, Phys. Lett. B **199**, 13 (1987); Z. Phys. A **331**, 123 (1988).
- [6] H. Arenhövel (private communication).
- [7] C. Herberg, Ph.D. thesis, Univ. Mainz, 1998; C. Herberg *et al.*, Eur. Phys. J. A **5**, 131 (1999).
- [8] D. R. Giebink, Phys. Rev. C **32**, 502 (1985).
- [9] M. Ostrick, Ph.D. thesis, Univ. Mainz, 1998.
- [10] J. Ahrens *et al.*, Nucl. Phys. News **2**, 5 (1994).
- [11] K. Aulenbacher *et al.*, Nucl. Instrum. Methods Phys. Res., Sect. A **391**, 498 (1997).
- [12] H. Schmieden, *Spin96: Proceedings of the 12th International Symposium on High-Energy Spin Physics, Amsterdam, 1996*, edited by C. W. de Jager *et al.* (World Scientific, River Edge, NJ, 1997).
- [13] R. Sprengard, Diploma thesis, Univ. Mainz, 1995.
- [14] J. Annand *et al.*, Nucl. Instrum. Methods Phys. Res., Sect. A **262**, 329 (1987).
- [15] M. Ostrick, Diploma thesis, Univ. Mainz, 1994.
- [16] From partial wave analysis of V. G. J. Stoks *et al.*, Phys. Rev. C **48**, 792 (1993).
- [17] T. Eden *et al.*, Nucl. Instrum. Methods Phys. Res., Sect. A **338**, 432 (1994).
- [18] T. N. Taddeucci *et al.*, Nucl. Instrum. Methods Phys. Res., Sect. A **241**, 448 (1985).
- [19] P. Grabmayr *et al.*, Nucl. Instrum. Methods Phys. Res., Sect. A **402**, 85 (1998).
- [20] H. Anklin *et al.*, Phys. Lett. B **428**, 248 (1998).
- [21] E. Bruins *et al.*, Phys. Rev. Lett. **79**, 5187 (1997); J. Jourdan *et al.*, Phys. Rev. Lett. **79**, 5186 (1997).
- [22] T. Eden *et al.*, Phys. Rev. C **50**, R1749 (1994).
- [23] M. Meyerhoff *et al.*, Phys. Lett. B **327**, 201 (1994).
- [24] J. Becker *et al.*, Ph.D. thesis, Univ. Mainz, 1998 (to be published).